Iranian Polymer Journal
16 (4), 2007, 219-232

Available online at: http://journal.ippi.ac.ir

A Micromechanics Approach for Fatigue of Unidirectional Fibrous Composites

Mahmood Zabihpoor* and Saeed Adibnazari

Department of Aerospace Engineering, Sharif University of Technology
P.O. Box: 11155/8639, Tehran, Iran

Received 31 August 2005; accepted 30 April 2007

ABSTRACT

The overall mechanical properties of composite materials are dependent on the mechanical response of individual constituents and their interactions while they may be relatively easy to determine. This paper represents a simulation process by which the cyclic stresses and fatigue loadings on its constituents could be predicted for an under fatigue loading lamina. Hence, the unidirectional composites fatigue would be studied through its constituents. The proposed model introduces a new coupled stiffness/strength technique by relating lamina stiffness to the stress field in its constituents. Therefore, the stress field and strength considerations in its constituents could be studied when the lamina stiffness is determined by a non-destructive process. For representing a complete description of the constituents' properties and their interactions, the effect of fibre/matrix interface debonding was introduced into the model. A number of experiments are conducted to verify the simulated relations. The comparison of theoretical and experimental predictions shows that the results are satisfactorily in good agreement.

Key Words:

fatigue;
stiffness degradation;
interfacial efficiency;
unidirectional composites.

(*) To whom correspondence to be addressed:
E-mail: zabihpoor@ae.sharif.edu

INTRODUCTION

Fibrous composites are finding more and more applications in aerospace, automotive, and naval industries. They have high stiffness and strength to weight ratio and good rating in regards to life time fatigue. On the other hand composite materials are anisotropic and their fatigue behaviours are very different from those behaviours exhibited by conventional materials. This is due to the damage process in composites which is significantly different from that observed in homogeneous and isotropic materials. Therefore, it is necessary to determine the relevant mechanical material response. The fatigue response of composite materials has been a subject of

active research in recent years. Four main damage modes have been observed in composites under fatigue loading: fibre/matrix debonding, matrix cracking, fibre fracture, and delamination [1].

To attain more efficient use of composite materials, damage models and life time prediction methodologies need to be improved continuously. based on the classification of fatigue criteria by Sendeckyj the fatigue models and life time predictions methodologies can be classified in four major categories: the macroscopic strength fatigue criteria, the criteria based on residual strength, and those based on residual stiffness, as well as the criteria based on the actual damage mechanisms [2].

In the last two decates, through the modelling of strength degradation, Charewicz et al. have assumed that the rate of reduction of residual strength is a function of life fraction [3]. Also Hahn et al. have proposed a model based on the assumption that residual strength degradation rate is inversely proportional to the residual strength [4]. A power law function of the number of cycles is assumed for the residual strength by Reifsnider et al. [5].

In stiffness degradation modelling, Hwang et al. have proposed a model to evaluate the life time prediction by using the stiffness degradation in a maximum strain failure criterion [6]. Sidoroff et al. have proposed a model for damage growth rate, where the damage variable is related to stiffness degradation [7]. The model was applied to the stress results from three point bending tests on glass/epoxy unidirectional composites under fixed load amplitude. Vieillevigne et al. have been adopted the model of Sidoroff and Subagio in terms of stress amplitude instead of strain amplitude [8].

Kawai has modified the model for off-axis fatigue of unidirectional carbon fibre reinforced composites [9]. Withworth has proposed a residual stiffness model for graphite/epoxy composites as a function of the ratio of applied cycles to fatigue life [10]. Yang et al. have developed a residual stiffness model for fibre dominated composite laminates [11]. They have also derived a statistical distribution of residual stiffness [12]. Indeed the model has been extended for matrix dominated composites which was applied to the fatigue behaviour of [±45] graphite/epoxy laminates. Also, Bröndsted et al. have extended stiffness reduction to life time prediction [13].

The predictions were based on experimental observation from wind turbine materials subjected to constant amplitude loading, variable amplitude block, and stochastic spectrum loading. Van Paepegem et al. implemented the model of Sidoroff and Subagio into a commercial finite element code [14]. To each gauss-point was assigned a state variable “D” which was related with the longitudinal stiffness loss. Shokrieh et al. have modified the residual strength model presented by Harris et al. and proposed a similar model for residual stiffness model as a function of number of cycles, applied maximum stress, and stress ratio in a normalized form [15].

Most of the proposed residual stiffness models are not valid in all three stages of stiffness degradation, especially if the stage of final failure is concerned [16]. In the residual stiffness approach, fatigue failure occurs when the modulus has degraded to a critical level which has been defined differently by many investigators. Therefore, to simulate the final failure, the strength properties must be included. On the other hand, destructive tests must be conducted for determining the residual strength of a lamina hence; various samples must be examined at different cycle numbers. Since the samples are not completely the same, there will be inherent dispersions in the test results and determination of the residual strength degradation behaviour. Therefore, coupling of these two approaches will be very useful and important in utilizing their advantages and removing the difficulties associated with each of them.

There are limited research works in the literature for stiffness/strength coupled models to use the stiffness degradation behaviour as a non-destructive fatigue parameter to overcome the final failure instant determination problem. Subramanian et al. have studied the concept of stiffness degradation behaviour [17]. They have shown that stiffness degradation could be quantitatively related to the residual strength of composite laminates through various models based on the observed damage. They have also used a micromechanics model in conjunction with the critical element scheme to predict the tensile fatigue life of laminated composites including the influence of fibre/matrix interface. This is one of the first known successful attempts to model the effect of fibre/matrix

interface on the tensile fatigue behaviour of composite laminates through stiffness/strength coupling.

Van Paepegem et al. have proposed a new coupled approach of residual stiffness and strength [16]. The stiffness/strength coupling is provided by introducing a modified static failure criterion and a macroscopic measure for damage in which composite material strength values are directly obtained from experiments on the lamina. Hence, the fatigue behaviour models can be classified in three major categories: fatigue life models; residual stiffness/strength models; fatigue damage modelling [18].

Fibre/matrix interface controls stress transfer between fibres and matrix, stress redistribution and hence mechanism of damage accumulation. It is shown that poor fibre/matrix bonding quality produces composite materials with poor mechanical properties [19]. Several studies have been conducted in recent years to determine the influence of fibre/matrix interface on the performance of fibre reinforced composites. The results of these studies show that interface affects composites toughness, strength, stiffness, fatigue resistance, and environmental stability [20-22]. In these investigations fibre surface treatment and fibre sizing have been considered to produce different levels of interface properties.

Afaghi-Khatibi et al. have investigated the effects of fibre/matrix interfacial adhesion on the fatigue residual strength of notched polymer matrix composite laminates [23]. They showed that the fatigue life of notched cross-ply laminates is sensitive to the level of adhesion between fibre and matrix. Gassan has studied the influence of interphase properties on the fatigue behaviour of composites [24]. The composites used were made of flax and jute yarns and wovens as reinforcements for epoxy resins, polyester resins, and polypropylene. High level of moisture absorption, poor wettability by non-polar plastics and insufficient adhesion between untreated fibres and the polymer resin in these natural fibre composites can lead to fibre/matrix debonding with aging.

Experimental studies have demonstrated the effect of fibre/matrix interface on the fatigue behaviour of carbon fibre and glass/epoxy cross-ply composites. It was found that fatigue performance is improved by increasing interface properties [25]. The quality of fibre/matrix adhesion was shown to have a significant effect on the fatigue behaviour of both reinforced brittle polyesters and ductile polypropylene. For both, the critical load for damage initiation was lower and damage propagation was more rapid for composites with untreated jute wovens. Also, Jia et al. have investigated the response of the interface bond under cyclic loading in fibre reinforced plastics by the ANN (Artificial Neural Network) method [25]. The model predictions and the results from experiments are satisfactorily in good agreement.

The most efforts being made, in the past were essentially macromechanical to simulate the fatigue behaviour. The main drawback in these models is that they cannot show the effect of interface imperfection in the selection of their constituents unless numerous fatigue tests were done on composites. Although several micromechanical simulations were performed previously for fatigue behaviour of unidirectional composites, these simulations ignored interface debonding effects and were not easy to apply [17,26].

This work presents a simulation process in which variation of stress fields in constituents can be predicted including the effect of fibre/matrix interface debonding under cyclic loading. In this way, a new coupled approach including the effect of fibre/matrix interface is proposed while it is easy to apply either.

MODELLING PROCEDURE

To investigate the fatigue of unidirectional composites through its constituents, a micromechanical approach was developed. By such a simulation procedure, the cyclic stresses induced in the constituents of a lamina could be determined when the lamina is subjected to fatigue loading.

The micromechanics approach was established based on bridging model however; the interfacial efficiency effect was not included in this model before. For this modelling we considered a conformation process in which lamina stiffness from the best described residual stiffness model would conform to that of the bridging micromechanics model. In this way, the parametric elements of the bridging matrix could be simulated as a function of cycle number, stress ratio, fibre volume fraction, stiffness of constituents, and interfacial efficiency. Therefore, a path

from lamina stiffness to the stresses (strength) of its constituents was introduced and a coupling stiffness/strength was established.

Micromechanical Simulation

The overall mechanical properties of composite materials are dependent on mechanical response of the individual constituents and their interactions, while it may be relatively easy to determine the mechanical properties of the individual constituents, as well as the comprehensive understanding and accurate consideration of their interactions. To determine such interactions, the following micromechanical simulation is used.

In the simulation process, the bridging micromechanics model is considered as a basis, in which the incremental stresses in the fibres are correlated with those in the matrix via eqn (1) [27].

$$\{d\sigma^m\} = [A]\{d\sigma^f\} \tag{1}$$

also, we have considered that for volume averaged stresses in a representative volume element (RVE) of the lamina [27] are determined by eqn (2).

$$\{d\sigma\} = V_f\{d\sigma^f\} + V_m\{d\sigma^m\} \tag{2}$$

by virtue of eqns (1) and (2) we can have:

$$\{d\sigma^f\} = (V_f[I] + V_m[A])^{-1}\{d\sigma\} \tag{3}$$

now, suppose that the fibres used are transversely isotropic and linearly elastic until rupture which have an incremental stress-strain relationship given by eqn (4) [28]:

$$\{d\varepsilon^f\} = [S^f]\{d\sigma^f\} \tag{4}$$

for the isotropic matrix, the constitutive equations are determined as in eqn (5) [28]:

$$\{d\varepsilon^m\} = [S^m]\{d\sigma^m\} \tag{5}$$

in which, $[S^f]$ and $[S^m]$ are the compliance of fibres and matrix, respectively. whereas the overall instantaneous compliance matrix of the lamina reads as eqn (6) [27]:

$$[S] = (V_f[S^f] + V_m[S^m][A])(V_f[I] + V_m[A\}])^{-1} \tag{6}$$

and the bridging matrix [A] is defined in the following form [26] in eqn (7):

$$[A] = \begin{bmatrix} a_{11} & a_{12} & a_{13} & a_{14} & a_{15} & a_{16} \\ 0 & a_{22} & a_{23} & a_{24} & a_{25} & a_{26} \\ 0 & 0 & a_{33} & a_{34} & a_{35} & a_{36} \\ 0 & 0 & 0 & a_{44} & a_{45} & a_{46} \\ 0 & 0 & 0 & 0 & a_{55} & a_{56} \\ 0 & 0 & 0 & 0 & 0 & a_{66} \end{bmatrix} \tag{7}$$

the independent elements of the bridging matrix are defined as follows [27]:

$$a_{11} = \frac{E_m}{E_f} \tag{8}$$

$$a_{22} = a_{33} = a_{44} = \frac{1}{2}(1 + \frac{E_m}{E_f}) \tag{9}$$

$$a_{55} = a_{66} = \frac{1}{2}(1 + \frac{G_m}{G_{12}^f}) \tag{10}$$

the dependent (off-diagonal) elements of the bridging matrix are determined by substitution of [A] into [S] and requiring the resulting overall compliance matrix of the composite [S] to be symmetric, i.e., $S_{ij}=S_{ji}$ and i,j= 1, 2, ..., 6 where the relations for the elements are developed for perfect bonding assumption.

According to the bridging micromechanics model, lamina mechanical properties could be explicitly determined based on the elements of the bridging matrix (a_{ij}). Since these relations are in general form based on a_{ij}, it is reasonable to modify the model for the imperfect bonding case through a new definition for a_{ij} based on the constituents properties and imperfection parameters.

First, it is necessary to modify the relations for elements which are affected by interface debonding through stiffness conformation process. Then reassembling modified bridging matrix, the stress field in the constituents will be obtained.

The following relation is derived for stiffness of the lamina with unidirectional fibre from the bridging micromechanics model [26]:

$$E_{11} = \frac{V_f + a_{11}V_m}{\left(\frac{V_f}{E_f}\right) + a_{11}\left(\frac{V_m}{E_m}\right)} \quad (11)$$

for a laminate which is subjected to cyclic loading, E_{11} varies as a function of n: cycle number, ó: stress level, and R: stress ratio, hence, $E_{11} = E_{11}(n,ó,R)$.

As it is known, the geometrical properties of a laminate, i.e., the fibre volume fraction, the fibre arrangement in the matrix, the fibre cross sectional shape, etc., do not change or only vary by negligibly small amounts [26]. Also it is reasonable to assume that the matrix and the fibre moduli do not change significantly [18,26]. Therefore, when E_{11} drops vs. cycles of loading, it may be assumed that V_f, E_f, and E_m are constant. Hence, based on the eqn (11), only a_{11} could be considered responsible for the lamina stiffness degradation under fatigue loading.

Stiffness Degradation Behaviour

Among the various stiffness degradation models the model proposed by Shokrieh et al. is a suitable choice. Because by using the normalization technique associated with this model, all different curves for different states of stress collapse to a single master curve [15].

According to this model, the stiffness degradation of the unidirectional lamina under fatigue loading is presented in the eqn (12):

$$\frac{E_{11} - E_{fi}}{E_{11_0} - E_{fi}} = \left[1 - \left(\frac{log(n) - log(n_0)}{log(n_{fi}) - log(n_0)}\right)^{\lambda}\right]^{1/\gamma} \quad (12)$$

where,

E_{11}: longitudinal stiffness of lamina at cycle number n

E_{110}: longitudinal stiffness of lamina at cycle number n_0

E_{fi} : longitudinal stiffness of lamina at final failure instant n_{fi}

ë and ã: experimental curve fitting parameters

For simplicity let ì =1/ã and $E_{11} = E_{11}(n,ó,R)$. All states of stress could be incorporated by adjustment of the curve fitting parameters ë and ã (or µ).

Conformation Process

In this section the main part of our work is explained. We have considered that the stiffness predictions from the residual stiffness model must be in conformance with those from the bridging model under fatigue loading. The left-hand side of eqn (12) shows normalized form of stiffness. This normalized stiffness could be obtained as a function of bridging matrix element "a_{11}" by substitution of stiffness prediction from the bridging model.

$$\frac{E_{11} - E_{fi}}{E_{11_0} - E_{fi}} = \frac{\frac{V_f + a_{11}V_m}{\left(\frac{V_f}{E_f}\right) + a_{11}\left(\frac{V_m}{E_m}\right)} - E_m}{\frac{V_f + a_{11_0}V_m}{\left(\frac{V_f}{E_f}\right) + a_{11_0}\left(\frac{V_m}{E_m}\right)} - E_m} \quad (13)$$

The interfacial efficiency determines how well the load is transferred from the matrix to the fibre. If the bonding is perfect and there is efficient load transfer from the matrix to the fibre, then $k \rightarrow 1$.To extend the bridging micromechanics model to include the effect of fibre/matrix interface imperfection, it is necessary to determine a_{11} vs. imperfection parameter which is defined as interfacial efficiency "k" in the literature. The left-hand side of eqn (12) is expressed vs. a_{11} in eqn (13). Hence to find a_{11} vs. k, we must determine the right-hand side of eqn (12) vs. "k". In this way, suppose that the fibre/matrix interfacial bonding efficiency varies vs. the loading cycle in the following form [17]:

$$k = A + B.log(n) \quad (14)$$

where "k" denotes interfacial efficiency as $0 \le k \le 1$, n is cycle number, and A and B are constant values.

Determination of Boundary Conditions

Reifsnider et al. have shown that as $k \rightarrow 1$, the stiffness of the unidirectional lamina approaches the value predicted by the rule of mixtures (R.O.M) and as $k \rightarrow 0$, it approaches the matrix modulus [17]. Thus, the interfacial efficiency manifests itself in the form of stiffness reduction in the unidirectional lamina. Therefore, the boundary conditions are:

k = 0 (full debonding) $E_{11} \rightarrow E_m$ (15)

k = 1 (perfect bonding) $E_{11} = E_m V_m + E_f V_f$ (16)

also, let us define:

$k = k_0$ at $n = n_0$ (17)

$k = k_{fi}$ at $n = n_{fi}$ (18)

substitution of eqns (17) and (18) into eqn (14) gives

$$B = \frac{k_{fi} - k_0}{log(n_{fi}) - log(n_0)} \quad (19)$$

and

$$A = k_0 \frac{log(n_{fi})}{log(n_{fi}) - log(n_0)} - k_{fi} \frac{log(n_0)}{log(n_{fi}) - log(n_0)} \quad (20)$$

finally,

$$k = k_0 \frac{log(n) - log(n_0)}{log(n_{fi}) - Log(n_0)} - k_{fi} \frac{log(n) - log(n_0)}{log(n_{fi}) - log(n_0)} \quad (21)$$

assuming that failure corresponds to full debonding, then $K_{fi} = 0$

$$k = k_0 \frac{log(n) - log(n_0)}{log(n_{fi}) - log(n_0)} \quad (22)$$

by re-arranging the eqn (22) we get eqn (23).

$$1 - \frac{k}{k_0} = 1 - \frac{log(n_{fi}) - log(n)}{log(n_{fi}) - log(n_0)} = \frac{log(n) - log(n_0)}{log(n_{fi}) - log(n_0)} \quad (23)$$

Simulation of Bridging Matrix Element

The right-hand side of eqn (23) completely appears in eqn (12) therefore, it is simple to re-arrange it versus "k" as follows

$$\frac{\frac{V_f + a_{11}V_m}{\left(\frac{V_f}{E_m}\right) + a_{11}\left(\frac{V_m}{E_m}\right)} - E_m}{\frac{V_f + a_{11_0}V_m}{\left(\frac{V_f}{E_m}\right) + a_{11_0}\left(\frac{V_m}{E_m}\right)} - E_m} = [1-(1-\frac{k}{k_0})^{\lambda}]^{\mu} \quad (24)$$

for finding the solution (a_{11} vs. k), let us assume power law function for $a_{11} = a_{11}(k)$

$$a_{11} = Dk^{\mu} + C \quad (25)$$

where "k" is the interfacial bonding efficiency and D, μ, and C are constants. Again, considering boundary conditions determined in the previous section:

(a) E_{11} approaches E_m when $k \to 0$ [17] (26)

on the other hand from the bridging micromechanics model:

$E_{11} \to E_m$ only when $a_{11} \to \infty$ (27)

therefore when "k" approaches zero; $a_{11} \to \infty$, substitution this condition into eqn (25) indicates that the value of "μ" is negative, hence

$$a_{11} = \frac{D}{k^{\mu}} + C \quad (28)$$

in which "μ" is redefined as a positive valued parameter.

(b) When k = 1 (perfect bonding) →

$E_{11} = E_m V_m + E_f V_f$ (R.O.M.)[17] (29)

from the bridging model for "E_{11}":

$E_{11} = E_m V_m + E_f V_f$ when $a_{11} = E_m/E_f$ (30)

substitution in eqn (25) gives

$$a_{11} = \frac{E_m}{E_f} = \frac{D}{(1)^{\mu}} + C \quad (31)$$

$$\Rightarrow D + C = \frac{E_m}{E_f} \quad (32)$$

re-writing for a_{11} reduces eqn (31) to eqn (33)

$$a_{11} = D(\frac{1}{k^{\mu}} - 1) + \frac{E_m}{E_f} \quad (33)$$

now, by substitution of a_{11} from eqn (33) into the eqn (13) gives

$$\frac{E_{11} - E_{fi}}{E_{110} - E_{fi}} = \frac{\frac{1}{E_f} + \frac{V_m}{E_m} M\left(\frac{1}{k_0^{\mu}} - 1\right)}{\frac{1}{E_f} + \frac{V_m}{E_m} M\left(\frac{1}{k^{\mu}} - 1\right)} \quad (34)$$

set the right-hand side of the eqn (34) vs. "k/k_0" (as an assumption) gives eqn (35)

$$\frac{\frac{1}{E_f} + \frac{V_m}{E_m} M\left(\frac{1}{k_0^{\mu}} - 1\right)}{\frac{1}{E_f} + \frac{V_m}{E_m} M\left(\frac{1}{k^{\mu}} - 1\right)} = \left(\frac{k}{k_0}\right)^{\mu} \quad (35)$$

by solving this equation, the two other simple equations will be obtained as follows:

$$(-DU_2 + U_1)k^{\mu} + (DU_2 - U_1)k_0^{\mu} = 0 \quad (36)$$

$$DU_2(k_0^{\mu} - k^{\mu}) = U_1(k_0^{\mu} - k^{\mu}) \quad (37)$$

where $U_1 = 1/E_f$ and $U_2 = V_m/E_m$. Both of the eqns (36)

and (37) give the same following result:

$$D = \frac{U_1}{U_2} = \frac{1}{1-V_f}\frac{E_m}{E_f} \quad (38)$$

also, from eqn (32) we can deduce

$$C = \frac{E_m}{E_f} - D = \frac{-V_f}{1-V_f}(\frac{E_m}{E_f}) \quad (39)$$

by comparing the eqns (35) and (24) for the case in which k_0=1, it is evident that if "k" is substituted by $[1-(1-k)^{\lambda}]$ thus, a_{11} will be changed as follows:

$$a_{11} = \frac{D}{[1-(1-k)^{\lambda}]^{\mu}} + C \quad (40)$$

by this conversion, the stiffness degradation model fully conforms to the bridging micromechanics model with a modified relation for a bridging matrix element.

$$\frac{E_{11}-E_{fi}}{E_{110}-E_{fi}} = [1-(1-k)^{\lambda}]^{\mu} = [1-(\frac{log(n)-log(n_0)}{log(n_{fi})-log(n_0)})^{\lambda}]^{\mu} \quad (41)$$

therefore, the main relation derived from this study will be as follows:

$$a_{11} = \frac{1}{V_m}\frac{E_m}{E_f}(\frac{1}{[1-(1-k)^{\lambda}]^{\mu}} - V_f) \quad (42)$$

since, the two other models for a_{11} were as follow as:

(1) $a_{11} = \frac{E_m}{E_f}$ (bridging micromechanics model and perfect bonding) [26] (43)

(2) $a_{11} = (1-k) + k\frac{E_m}{E_f}$ (general model of a_{11}) [29] (44)

EXPERIMENTAL

In this section a short description is given of the static and fatigue experiments, whose results will be compared against the proposed modelling.

Test Programme

To verify the simulated relation, it is necessary to conduct some experiments. A number of static tensile tests were performed to determine mechanical property of manufactured unidirectional composites in fibre direction. Then, tension-tension fatigue tests were conducted for the same composite material, through which stiffness degradation of the material could be determined experimentally. As another result of the fatigue tests performed, the constants ã, ë, ì in stiffness model may be calculated. Therefore, the values of the bridging matrix element a_{11} could be predicted both from the proposed model and from the substitution of experimental stiffness in bridging micromechanics model. The comparisons represent the accuracy of the simulated relation and predicted behaviour. Hence, the power law relation suggested for a_{11} would be approved.

Materials

The material used was a unidirectional glass/epoxy composite. The fibre is E-glass 92145 Cs-Interglass and the epoxy is Rutapox L20 with the hardener SL (Bakelite EPR L20-EPH 960). The main sheet of the test samples is stacked in ten layers. The fibres direction of all layers is aligned in the same direction of the applied load. Mechanical properties of the unidirectional glass/epoxy (92145/L20-SL) composite and its constituents are obtained through material characterization tests are listed in Table 1.

For such a material, the thickness of ten layers laminate after curing is equal to 2 mm. This thickness value is in the standard range which is recommended in ASTM D 3039 for composites tension tests. All composite specimens are manufactured using hand lay-up method. The samples were cut to dimensions recommended in ASTM D 3039 by a diamond saw. The dimensions and configuration of samples are presented in Table 2 and Figure 1, respectively. Figure 2 shows a unidirectional test sample before static tensile and fatigue tests.

Static tensile tests were conducted for characterizing the manufactured unidirectional laminate. Based on such tests, the unidirectional lamina initial stiffness and strength were determined (Table 1). More than five specimens were used for static tests. All test requirements were considered for static tests according to ASTM D 3039.

The laminate (lamina) fibre volume fraction was determined by the ignition loss method (ASTM D 2584). The value of fibre volume fraction was obtained as V_f = 0.45 as mentioned in Table 1. Similar

Table 1. Results of static tensile tests on the unidirectional glass/epoxy (92145/L20-SL) composite and its constituents.

Property / Material	$E = E_{Exp}(0.25)$ [MPa]	σ_{ult} [MPa]	υ	V_f	E_m [MPa]	E_f [MPa]
UD. Glass/Epoxy [92145/L20]	37215.5	589.8	0.237	0.45	2.91	73

samples were used to determine the stiffness degradation versus cycles. All fatigue tests requirements were based on ASTMs D 3479 and D 3039.

Testing Machine

An Instron testing machine (series 8500) was employed for performing static and fatigue tests. This type of testing machine was equipped with hydraulic grips. The grip pressure was set at 20 bars for static and fatigue tests on the tabs of the samples.

The speed of cross-head of the machine was 1.5 mm/min for static and 5.8 Hz for fatigue loading. The wave form of loading in fatigue tests was selected to be sine wave with the stress ratio R = 0.1.

RESULTS AND DISCUSSION

It is advantageous to use stiffness changes in the simulation procedure because determination of stiffness is a non-destructive process in any instant and can remove the necessity of conducting tests on various samples. Hence, this may decrease the scattering of the test results. In this way, the cost and time needed for conducting the tests will be diminished.

In this work, the framework for deviation of an extended micromechanics model conforms to the theoretical stiffness degradation on an experimental stiffness degradation model. The final relations for the bridging matrix element yield complete conformance between theoretical and experimental stiffness changes. Also this relation (a_{11} vs. k) includes the same constant parameters introduced in the experimental stiffness degradation model, and no additional constant appears in the simulated relation. Hence, no further experiments are needed in order to determine a_{11} values. Using the proposed model, lamina stiffness relates to stress field in constituents. Hence, a new coupled stiffness/strength model is introduced.

Although the equatios are a little more complex than before, they are yet easy to apply. Figures 3 and 4 represent the curves which are provided on the basis of the recent simulation of a_{11} and a general relation of a_{11} vs. k. Mechanical properties of constituents are selected from reference No. 30 in which E_m = 4.6 GPa for epoxy matrix and E_f = 235 GPa for AS4 fibres. Also, the value of fibre volume fraction in the lamina is equal to V_f = 0.4. On the other hand the values of experimental curve fitting parameters for such a material system are extracted from reference No. 15 where ë = 14.573 and ì = 3.3069. To show the sensitivity of the model predictions with respect to variations of ë and µ, the curves are drawn for different values of ë and a constant value of µ in Figure 3. Similarly, the curves are plotted for different values of µ and a constant value of ë.

Table 2. Dimensions of test samples (in mm, angle in degree).

L_T	L_{tab}	W	$t_{specimen}$	t_{tab}	θ
350	60	12.7	1.9	5	15

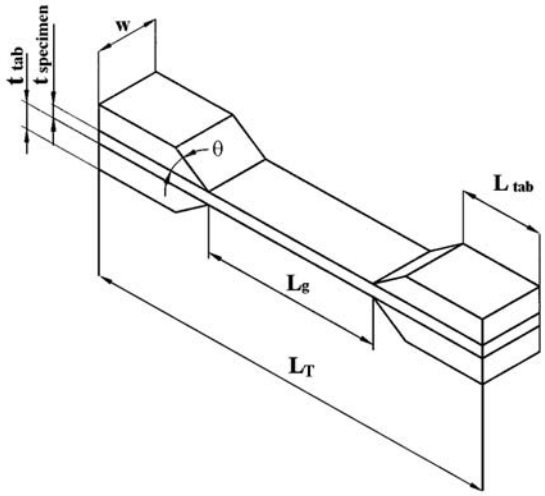

Figure 1. Configuration of test samples.

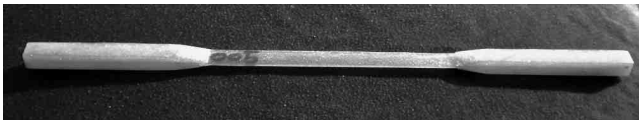

Figure 2. Unidirectional test sample for tensile static and fatigue test.

Based on the curves shown in Figures 3 and 4, a_{11} values are more sensitive to λ than μ. By decreasing the value of λ or increasing the value of μ, the curves move to the left as well as upwards. Moreover, the value of "k_g" increases while the value of λ decreases or the value of μ increases, where "k_g" is the value of "k" corresponding to the point at which the change in the a_{11} value starts.

By applying this model, the stress field would be predicted in the composite's constituents. Also, residual strength "R_S" of the composite material could be found based on the failure criteria of fibres or matrix. However, the assumption of "the final failure corresponds to interface debonding" gives an upper band value of "R_S". As is shown in Figures 3 and 4 there are great differences between the a_{11} values which are obtained from two different models. Hence, corrected a_{11} values could result in significantly different cyclic stress fields in composite's constituents through modified bridging matrix [A].

It is of interest to note that in the basic bridging model a_{11} is only a function of E_m and E_f , i.e., a_{11}= a_{11} (E_m, E_f). In the general linear model, a_{11} is dependent on E_m, E_f, and also "k", i.e., a_{11}= a_{11} (E_m, E_f, k). Finally in the modified model, a_{11} is introduced as a function of E_m, E_f, k, and V_f , i.e., a_{11}= a_{11} (E_m, E_f, k, V_f) which may be considered as a complete description of a_{11}. Also for all models a_{ij} elements are non-

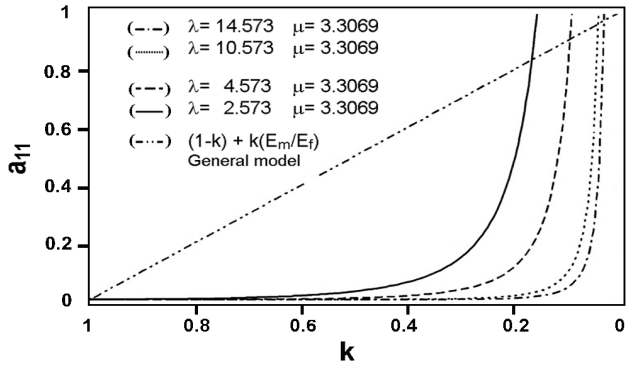

Figure 3. The plot of a_{11} vs. k for two different models (μ=cote and different values of λ).

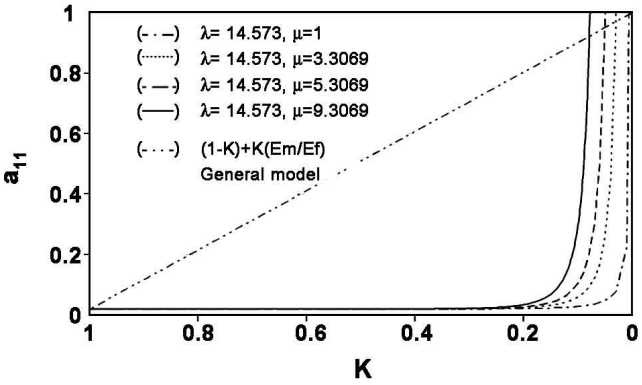

Figure 4. The plot of a_{11} vs. k for two different models (λ=cote and different values of μ).

dimensional parameters. To explain the effect of V_f in a_{11} values, the model is rewritten in the following form, let us define

$$S = \frac{1}{(1-(1-k)^{\lambda})^{\mu}} - 1 \tag{45}$$

in which

$$0 \le k \le 1 \Rightarrow \qquad 0 \le S < \infty \tag{46}$$

hence, a_{11} will be expressed vs. S, V_m(or V_f), E_m and E_f as:

$$a_{11} = (1+\frac{S}{V_m})\frac{E_m}{E_f} \tag{47}$$

substituting V_m= 1-V_f in eqn (47) gives

$$a_{11} = (1+\frac{S}{1-V_f})\frac{E_m}{E_f} \tag{48}$$

for convenience

$$\eta = \frac{S}{V_m} = \frac{S}{1-V_f} \tag{49}$$

therefore,

$$a_{11} = (1+\eta)\frac{E_m}{E_f} \tag{50}$$

by decomposing a_{11} in two distinct parts

$$a_{11} = a_{11_{Perfect}} + a_{11_{Prog}} \tag{51}$$

in which

$$a_{11_{perfect}} = \frac{E_m}{E_f} \qquad \text{(according to Huang's Model for perfect bonding)} \tag{52}$$

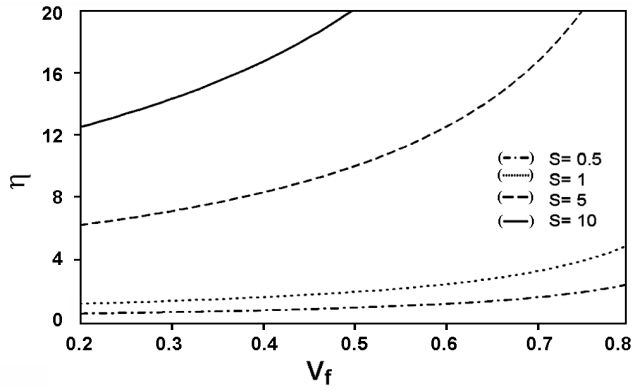

Figure 5. The plot of normalized a_{11} vs. V_f .

and

$$a_{11_{Prog}} = \frac{S}{1-V_f}\left(\frac{E_m}{E_f}\right) = \eta \frac{E_m}{E_f} \qquad (53)$$

Finally Normalized a_{11} could be defined as

$$\eta = \frac{a_{11} - a_{11_{Perfect}}}{a_{11_{Perfect}}} \qquad (54)$$

The above expression explains the effect of interface debonding progress. We named the coefficient "η" as "interface imperfection effect". Figure 5 shows the plot of normalized a_{11} vs. V_f and describes the dependency of a_{11} to V_{11}. The graph in this figure indicates that a_{11} is highly dependent on V_f especially for higher values of "S" which correspond to lower values of interface bonding efficiency "k". On the other hand, lower values of "k" produce higher values of "S" and finally higher values of interface imperfection coefficient "η". This means that the dependency of a_{11} on V_f increases while interface debonding grows. Therefore, $a_{11_{prog}}$ is an important term which must be considered

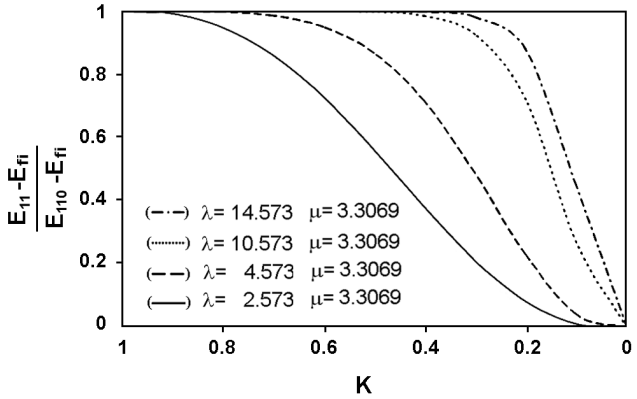

Figure 6. Stiffness degradation vs. k for different values of λ and a typical value of μ.

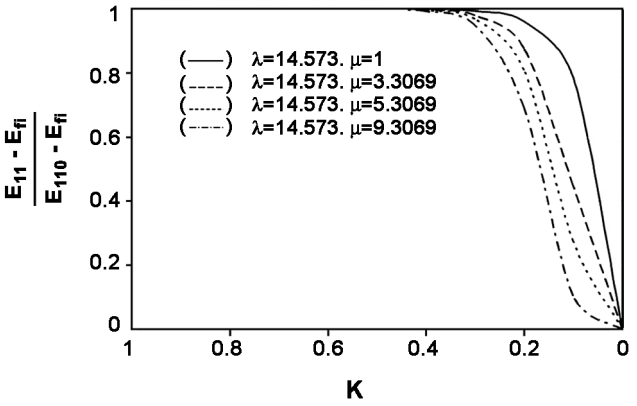

Figure 7. Stiffness degradation vs. k for different values of μ and a typical value of λ.

in the calculations. The simulated relation in this paper involves such considerations and gives a complete description of a_{11}.

As it is mentioned, λ and γ are important parameters for the stiffness degradation model. The stiffness degradation dependencies on λ and γ (μ) are shown in Figures 6 and 7. However, by comparing Figures 6 and 7 with Figures 3 and 4 it can be inferred that the sensitivity of the simulated behaviour of a_{11} with respect to variations of λ and μ is not as much as that for stiffness degradation. Therefore, the values of λ and μ are less important for a_{11} than for stiffness degradation behaviour. This could be explained by the level of sensitivity of E_{11} to a_{11} as follows, the dependency of E_{11} to a_{11} as was described in the micromechanics model by eqn (11) magnifies the effects of λ and μ in the determination of E_{11}. Hence, it is acceptable to obtain these values through approximations when these parameters cannot be determined precisely. It is interesting to note that

$$k=1 \Rightarrow [1-(1-k)^{\lambda}] = 1 \qquad (55)$$

and

$$k=0 \Rightarrow [1-(1-k)^{\lambda}] = 0 \qquad (56)$$

therefore, the limits of previous and current variables "k" and "1-(1-k)$^{\lambda}$" remain unchanged.

By the recent relation for a_{11}, boundary values of

Figure 8. Unidirectional test sample after tensile static test.

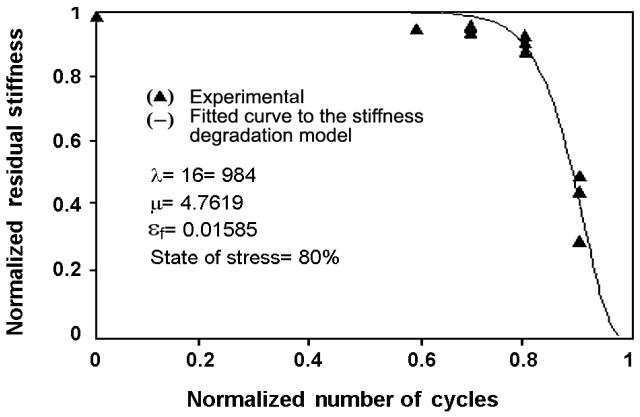

Figure 9. Stiffness degradation of the unidirectional composites during experiments.

E_{11} are fully satisfied and the values of μ, λ, and V_f determine the rate of variations, but none of them were incorporated in general modification.

As explained in the experimental section, to verify the simulated behaviour of a_{11}, a number of static and fatigue tests were conducted. The results of static tensile and volume fraction tests on the unidirectional glass/epoxy composite are listed in Table 1, where $E_{Exp(0.25)}$ corresponds to experimental lamina stiffness from static test n = 0.25.

Figure 8 shows the sample test after tensile static tests. As the observed fibre/matrix debonding is the primary failure mode of the sample. Thus, the material selected will be a good candidate for evaluating the proposed model if the same failure mode occurs for the material under fatigue loading.

The stiffness degradation of the unidirectional composite is presented in Figure 9 in which normalized residual stiffness and normalized number of cycles are

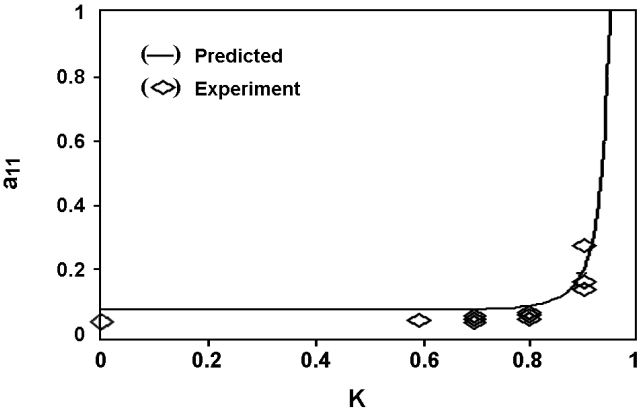

Figure 10. Variation of a_{11} vs. k (comparisons of experiments and model predictions).

Figure 11. Unidirectional test sample after tension-tension fatigue test.

the normalized terms in left- and right-hand sides of eqn (12), respectively. Through fatigue experiments and the behaviour shown, the material constants λ and μ are obtained as 16.984 and 4.7619, respectively. These values of material constants are used in the proposed model for predicting the values of a_{11}. On the other hand, by substitution of the stiffness value of the laminate at any cycle in eqn(11) (the relation of E_{11} vs. a_{11}), the value of a_{11} at corresponding cycle would be found. Hence, the variation of a_{11} vs. n could be drawn according to experimental stiffness and model predictions. Figure 10 represents the comparisons of a_{11} obtained form the model predictions and the experiments.

As it can be observed, the behaviours predicted by the model are similar to the experimental ones. Therefore, the power law assumed for a_{11} is approved here. The small differences between a_{11} values from theoretical and experimental methods are mainly due to approximate values of material constants λ and μ from experimental stiffness degradation. Since, the inherent scatterings in test results are involved in the process of determination of these constants.

Figure 11 represents the unidirectional test sample data after fatigue test. As it is shown, similar to static tests, the primary failure mode in the material system is fibre/matrix debonding. Thus, the response of the selected material under fatigue loading could be used to evaluate successfully the simulated relation and the assumptions associated with the model which is close to real state occurred for the material in experiments.

CONCLUSION

A micromechanics model for fatigue of unidirectional composites has been proposed. The simulated relation represents complete description of bridging matrix element versus constituents modulus, interfacial efficiency, and fibre volume fraction. The model was derived from average stresses in constituents and gave

an upper band value for residual strength. Complete conformation of extended bridging matrix element with empirical stiffness degradation model indicates that both could predict similar mechanical behaviour of materials. Sensitivity of the model to the values of material constants (λ and μ) are less than for stiffness degradation behaviour. Also, highly nonlinear behaviour has been observed in extended bridging matrix element a_{11} vs. k. The proposed model introduces a new coupled stiffness/strength technique by relating lamina stiffness to stress field in constituents. Hence, the stress field and strength consideration in constituents could be studied when the lamina stiffness was determined by a non-destructive process. Comparisons of the theoretical and the experimental predictions indicate that the results are satisfactorily in good agreement with each other which approves the power law assumption in the model.

ACKONWLEDGEMENTS

The authors are grateful to Ramisa Rezaei for her technical comments.

NOMENCLATURE

A, B, C, D	Constant values
a_{ij}	Elements in bridging matrix
a_{11_0}	a_{11} at n_0
$a_{11_{Perfect}}$	a_{11} for perfect bonding assumption
$a_{11_{Prog}}$	a_{11} as debanding grows
E_f	Fibre elastic modulus
E_{fi}	Longitudinal stiffness of lamina cycle "n_{fi}"
E_m	Matrix elastic modulus
E_{11}	Lamina longitudinal elastic modulus
E_{110}	Static elastic modulus(E_{11} at n_0)
G^f_{12}	Fibre shear modulus
G_m	Matrix shear modulus
k	Interfacial efficiency
k_{fi}	Interfacial efficiency at "n_{fi}"
k_g	Corresponding "k" to the point at which the change in the a_{11} value starts
k_0	Interfacial bonding efficiency corresponding to "n_0"
n	Cycle number
n_{fi}	Number of cycles to failure
n_0	Initial number of cycles
R	Stress ratio; $R= \sigma_{min}/ \sigma_{max}$
R_S	Residual strength
S	Intermediate parameter related to "k"
U_1	Intermediate parameter related to "E_f"
U_2	Intermediate parameter related to "E_m, V_m"
V_f	Fibre volume fraction
V_m	Matrix volume fraction
[A]	Bridging matrix
[S]	Overall instantaneous compliance matrix
$[S^f]$	Compliance of fibre
$[S^m]$	Compliance of matrix
γ, λ, μ	Material constants
η	Interface imperfection effect
σ	Stress level
$d\sigma$	Incremental stress in the lamina
$d\sigma^f$	Incremental stress in the fibre
$d\sigma^m$	Incremental stress in the matrix
R.O.M	Rule of mixtures
RVE	Representative volume element

REFERENCES

1. Stinchcomb W.W., Reifsnider K.L., Yeung P., Masters J., Effect of ply constraint on ftigue damage development in composite material laminates, In: *Fatigue of Fibrous Composite Materials*, Lauraitis K.N. (Ed.) ASTM STP 723, American Society for Testing and Materials, Philadelphia, 64-84, 1981.
2. Sendeckyj G.P., Life prediction for resin-matrix composite materials. In: *Fatigue of Composite Materials*, Reifsnider K.L. (Ed.), Elsevier Science, Amsterdam, 431-483, 1991.
3. Charewics A., Daniel I.M., Damage mechanics and accumulation in graphite/epoxy laminates. In: *Composite Materials: Fatigue and Fracture*, Hahn H.T. (Ed.), ASTM STP 907, American Society for Testing and Materials, Philadelphia, 274-297, 1986.
4. Hahn H.T., Kim R.Y., Fatigue behavior of composite laminates, *J. Compos. Mater.*, **10**, 156-180, 1976.
5. Reifsnider K.L., Stinchcomb W.W., A critical element model of the residual strength and life of fatigue-loaded composite coupons. In: *Composite Materials: Fatigue and Fracture*, Hahn H.T. (Ed.),

ASTM STP 907, American Society for Testing and Materials, Philadelphia, 233-251, 1986.
6. Hwang W., Han K.S., Fatigue of composite materials-damage model and life prediction, composite materials: Fatigue and fracture, Lagace P.A. (Ed.), 2nd Volume, ASTM STP 1012, American Society for Testing and Materials, Philadelphia, 87-102, 1989.
7. Sidoroff F., Subagio B., Fatigue damage modeling of composite materials from bending test, *Proc. Int. Conf. Compos. Mater. (ICCM-VI) & 2nd Eur. Conf. Compos. Mater. (ECCM-II*), Vol. 4, London, 4.32-4.39, 20-24 July, 1987.
8. Vieillevigne S., Jeulin D., Renard J., Sicot N., Modelling of fatigue behaviour of a unidirectional glass epoxy composite submitted to fatigue loadings, *Proc. Int. Conf. Fatig. Compos.*, la societe Francaise de Metallurgie et de Materiaux, Paris, 424-430, 3-5 June, 1997.
9. Kawai M., Damage mechanics model for off-axis fatigue behaviour of unidirectional carbon fibre-reinforced composites at room and high temperatures, *Proc. 12th Int. Conf. Compos Mater., (ICCM-12)*, Paris, 322-325, 5-9 July, 1999.
10. Withworth H.A., Modelling stiffness reduction of graphite epoxy composite laminates, *J. Compos. Mater.*, **21**, 362-372, 1987.
11. Yang J.N., Jones D.L., Yang S.H., Meskini A., A stiffness degradation model for graphite/epoxy laminates, *J. Compos. Mater.* **24**, 753-769, 1990.
12. Yang J.N., Lee L.J., Sheu D.Y., Modulus reduction and fatigue damage of matrix dominated composite laminates, *Compos. Struct.*, **21**, 91-100, 1992.
13. Bröndsted P., Andersen S.I., Lilholt H., Fatigue damage accumulation and life time prediction of GFRP materials under block loading and stochastic loading, *Proc. 18th Risö Int. Symp. Mater. Sci.*, Roskilde, 269-278, 1-5 Sep.,1997.
14. Van Paepegem W., Degrieck J., Numerical modeling of fatigue degradation of fibre-reiforced composite materials, *Proc. 5th Int. Conf. Comput. Struct. Technol., Vol. F: Comput. Tech. . Mater., Compos. Compos. Struct.*, Leuven, 319-326, 6-Sep. 2000.
15. Shokrieh M.M., Lessard L.B., Fatigue under multiaxial stress systems, In: *Fatigue in Composites*, Harrris B. (Ed.), CRC Press, Boca Raton, Ch.3, 63-109, 2003.
16. Van Paepegem W., Degrieck J., A new coupled approach of residual stiffness and strength for fatigue of fibre-reinforced composites, *Int. J. Fatigue*, **24**, 747-762, 2002.
17. Subramanian S., Reifsnider K.L., Stinchcomb W.W., A Cumulative damage model to predict the fatigue life of composite laminates including the effect of a fibre-matrix interphase, *Int. J. Fatigue*, **17**, 343-351, 1995.
18. Degrieck J., Van Paepegem W., Fatigue damage modelling of fibre-reinforced composite materials: Review, *Appl. Mech. Rev.*, **54**, 279-300, 2001.
19. Mullin J.V., Influence of fibre property variation on composite failure mechanisms. In: *Analysis of Test Methods for High Modulus Fibres and Composites*, Whitney J.M. (Ed.), ASTM STP 521-EB, American Society for Testing and Materials, San Antonio, 349-366, 1972.
20. Drzal L.T., Composite interphase characterization, *SAMPE J.*, **19**, 7-13, 1983.
21. Shih G.C., Ebert L.J., The effect of the fibre/matrix interface on the flexural fatigue performance of unidirectional fibre glass composites, *Compos. Sci. Technol.*, **28**, 137-61, 1987.
22. Zhou L.M., Kim J.K., Mai Y.W., Micromechanical characterization of fibre/matrix interfaces, *Compos. Sci. Technol.*, **48**, 227-36, 1993.
23. Khatibi A.A., Ye L., Mai Y.W., An experimental study of the influence of fibre/matrix interface on fatigue tensile strength of notched composite laminates, *Compos. Part B-Eng.*, **32**, 371-377, 2001.
24. Gassan J., A study of the fibre and interface parameters affecting the fatigue behaviour of natural fibre composites, *Compos. Part A-Appl. S.*, **33**, 369-374, 2002.
25. Jia J., Davalos J.F., An artificial neural network for the fatigue study of bonded FRP-wood interfaces, *Compos. Struct.*, **74**, 106-114, 2006.
26. Huang Z.M., Micromechanical modeling of fatigue strength of unidirectional fibrous composites, *Int. J. Fatigue*, **24**, 659-670, 2002.
27. Huang Z.M., The mechanical properties of composite reinforced with woven and braided fabrics, *Compos. Sci. Technol.*, **60**, 479-498, 2000.
28. Huang Z.M., A unified micromechanical model for the mechanical properties of two constituent com-

posite materials. Part I: Elastic behavior. *J. Thermoplast. Compos.*, **13**, 452-271, 2000.
29. Zabihpoor M., Adibnazari S., Abedian A., Evaluation and development of bridging micromechanics model using mechanical properties from composite materials characterization tests, *Iran. J. Polym. Sci. Technol. (in Persian)*, **18**, 369-376, 2006.
30. Niu M.C.Y., *Composite Airframe Structures, Practical Design Information, and Data*, Conmilit Press LTD., Washington, Ch.2, 1992.